Poultry Science®

Dietary supplementation of poly-dihydromyricetin-fused zinc nanoparticles alleviates fatty liver hemorrhagic syndrome by improving antioxidant capacity, intestinal health and lipid metabolism of laying hens

Yuanting Yang ,*,[1] Xugang Shu,† Hafiz Umer Javed,‡ Qun Wu,* Hu Liu,* Jiancheng Han,*,[1] and Hanlin Zhou*,[2]

*Zhanjiang Experimental Station, Chinese Academy of Tropical Agricultural Sciences, Zhanjiang 524013, China; †College of Chemistry and Chemical Engineering, Zhongkai University of Agricultural Engineering, Guangzhou 510225, China; and ‡Guangxi College and University Key Laboratory of High-Value Utilization of Seafood and Prepared Food in Beibu Gulf, College of Food Engineering, Beibu Gulf University, Qinzhou 535011, China

ABSTRACT Fatty liver hemorrhagic syndrome is the main cause of noninfectious death of laying hens and results in substantial economic losses to the poultry industry. This study focused on evaluating the effects of Poly-dihydromyricetin-fused zinc nanoparticles (**PDMY-Zn NPs**) on antioxidant capacity, liver lipid metabolism, and intestinal health in laying hens. A total of 288 Jingfen laying hens (52 wk old) with similar body weights were randomly divided into 4 dietary groups with 6 replicates in each group for 8 wk. The control group received a basal diet, while the treatment groups were supplemented with PDMY-Zn NPs at levels of 200, 400, and 600 mg/kg, respectively. The results indicate that PDMY-Zn NPs supplementation can enhance antioxidant parameters ($P < 0.05$) in the blood and liver of laying hens. Simultaneously, it can mitigate vacuolar degeneration and inflammatory necrosis in hepatocytes, improve the relative expression level of related parameters associated with liver lipid metabolism and key regulatory genes ($P < 0.05$). Furthermore, it has been observed to reshape the composition and diversity of cecum microbes by increasing beneficial probiotics such as *Lactobacillus* and *Prevotella*, while also enhancing villi height and villi/crypt ratio in the duodenum and ileum ($P < 0.05$). Additionally, it elevates liver bile acid content along with the relative expression of key genes involved in liver synthesis ($P < 0.05$). In summary, PDMY-Zn NPs showed potential to alleviate fatty liver hemorrhagic syndrome by enhancing antioxidant capacity, regulating liver lipid metabolism, and maintaining intestinal health.

Key words: dihydromyricetin, laying hen, lipid metabolism, antioxidant, fatty liver hemorrhagic syndrome

2024 Poultry Science 103:104301
https://doi.org/10.1016/j.psj.2024.104301

INTRODCTION

Chronic liver disease (**CLD**) is a leading cause of mortality and morbidity worldwide (Patten and Shetty, 2018). Nonalcoholic fatty liver disease has become the most common CLD in humans (global prevalence exceeds 30%) and is closely associated with increased mortality from cardiovascular disease, extrahepatic cancer and liver complications (Powell et al., 2021; Younossi et al., 2023). Fatty liver hemorrhagic syndrome (**FLHS**) is one of the common CLD in laying hens, which has great similarity with Nonalcoholic fatty liver disease (Hamid et al., 2019) . In addition, FLHS is the leading cause of noninfectious mortality in cage laying hens worldwide, mainly manifested by significant decrease in egg production, liver steatosis and sudden death, etc., bringing great economic losses to the laying industry (Trott et al., 2014; Tu et al., 2023). Although caused by a variety of factors such as nutrition, hormones, environment and metabolism, oxidative stress is generally recognized as a major factor in the pathophysiology of CLD (Arroyave-Ospina et al., 2021; Gao et al., 2019). Moreover, it plays a crucial role in further progression to hepatic fibrosis, cirrhosis, and hepatocellular carcinoma (Allameh et al., 2023). Therefore, it is necessary to adopt appropriate strategies to reduce the adverse consequences caused by excessive oxidative stress in laying hens.

Natural products, primarily compounds derived from plant, animal and mineral sources, have been an important resource for maintaining health and treating or preventing human and animal diseases over millennia

Received June 27, 2024.
Accepted September 3, 2024.

[1]These authors contribute equally.
[2]Corresponding author: Zhouhanlin8@163.com

(Mehta et al., 2015). There has been substantial evidence that dietary supplementation of natural products with antioxidant, inflammatory and lipid-lowering components can effectively reduce liver damage caused by FLHS (Xing et al., 2020; Gao et al., 2020; Miao et al., 2021). Overall, their effects are mainly related to regulating glucose and lipid metabolism, alleviating oxidative stress and inflammation, and improving gut microbiota and metabolites. However, the underutilized benefits of natural products are attributed to their poor water solubility, low permeability, instability and high metabolic rate (Meena et al., 2020). Currently, this problem can be solved by increasing its bioavailability through cyclodextrin complexation, solid-lipid nanoparticles, liposome and polymeric nanoparticles, etc (Paroha et al., 2020; Vanti et al., 2021) .

Dihydromyricetin (**DMY**), a naturally occurring flavonoid compound primarily extracted in the traditional chinese medicinal plant "*Ampelopsis grossedentata*"(-Chen et al., 2021a). Studies have shown that it has many activities, such as oxidation resistance, anti-inflammatory, antimicrobial, hepatoprotective, and antitumor activity (Wu et al., 2022; Zhang et al., 2022). Several studies have shown that DMY can mitigate hepatic steatosis or damage caused by various stresses by improving lipid metabolism, enhancing antioxidant capacity, and inhibiting inflammation reaction (Xie et al., 2016; Dong et al., 2019; Silva et al., 2020). Interestingly, the DMY molecular structure has upper supramolecular stability, an integral conjugated large *pi* bond, strongly coordinated oxygen atoms, and appropriate molecular compositions, which can react to form DMY-metal complexes with the metal ions (Zhang et al., 2005). It is rather surprising that DMY has shown better biological activity in the presence of metal ions (Liu et al., 2019).

The trace mineral zinc (**Zn**) is a vital component of the laying hen's diet that plays a number of physiological roles, including cell growth and differentiation, immune regulation, and protein and carbohydrate metabolism (Abd El-Hack et al., 2017). Zn also plays a role in the proper function of lipid and glucose metabolism, regulation and formation of insulin expression (Olechnowicz et al., 2018). Moreover, it has the effects of alleviating environmental stress (Zhu et al., 2017), reducing aggressive behavior of laying hens (Sorosh et al., 2019), and maintaining egg quality and laying performance (Cufadar et al., 2020). Therefore, our previous studies have prepared Poly-dihydromyricetin-fused zinc nanoparticles (**PDMY-Zn NPs**) with the chemical combination of Zn and DMY (Luo et al., 2021). By characterization, it formed 300-400nm irregular brown powder, and had good thermal stability and gastrointestinal stability (Luo et al., 2021). Similar studies have also shown that it has stronger scavenging activity on DPPH, hydroxyl radicals, and paraffin on superoxide anion radical than vitamin C (Wu et al., 2011). Moreover, our recent findings showed that compared with other zinc sources, PDMY-Zn NPs have the potential effect of improving lipid metabolism and reducing the incidence of FLHS in laying hens (Yang et al., 2022). However, the appropriate level of PDMY-Zn NPs supplementation and possible mechanisms to alleviate FLHS in laying hens have not been clarified. Hence, the present study aimed to examine the effects of different levels PDMY-Zn NPs on lipid metabolism, serum biochemical, and antioxidant indices, intestinal health and bile acid metabolism of laying hens.

MATERIALS AND METHODS

Preparation of PDM-Zn NPs

DMY product was extracted from *Ampelopsis grossedentata*. In brief, dried leaves of *Ampelopsis grossedentata* were weighed and dissolved completely in a beaker with deionized water ata 1:20 solid-liquid ratio. After reaction for 30 min at 100°C and pH=5, the filtrate was collected and refrigerated at -4°C to produce crystallization. After filtration, the collected solids were soaked in ethanol (anhydrous) for further purification. Subsequently, after repeated filtration with deionized water lotion for several times, the collected DMY samples were air-dried at 50°C. The prepared DMY and $ZnSO_4$ were fully dissolved respectively and mixed according to the molar ratio of 2:1. After reaction at 70°C and pH = 6.4 for 4 h, the particles were filtered and collected while hot, and then washed repeatedly with deionized water and ethanol. Finally, PDM-Zn NPs (DMY, 80.37%; Zn, 19.63%) was dried in a hot air oven at 50°C. The detailed synthesis and characterization of PDM-Zn NPs can be seen in the previous studies of our research group (Luo et al., 2021).

Experimental Design and Management

Experimental protocol was approved by Ethics and Welfare of Animal Experiments Committee of Zhongkai University of Agriculture and Engineering, China (Approval no:20220413-02). Two hundred eighty-eight Jingfen pink-shell laying hens (52-wk-old) with similar weight were randomly selected and assigned to 4 dietary treatments, with 6 replicates of 12 hens each. The control group (T0) was fed the basal diet, while the T200, T400, and T600 treatment groups were fed the basal diet supplemented with 200, 400, and 600 mg/kg of PDM-Zn NPs, respectively. The basal diet (Table 1) was formulated to meet all nutritional requirements except Zn according to the basic requirements of National Research Council (1994) and China Agricultural Standard (NY/T 33-2004). Zn was added to the basal diet in the form of PDM-Zn NPs. The actual concentrations of Zn in the diets of each group were 37.40, 78.73, 119.91 and 160.98 mg/kg, respectively, determined by inductively coupled plasma emission spectrometry .

All birds were raised in an experimental farm and housed in 3-tier ladder-type cages (60 × 50× 50 cm) with 3 hens per cage. These hens were fed 105 grams per day (twice a day, at 5:30 a.m. and 4:30 p.m.), water ad

Table 1. Ingredient and nutrient composition of the basal diets.

Ingredients	Content %
Corn	59.50
Soybean meal	23.52
Soybean oil	2.09
Limestone	9.37
Corn gluten meal	2.99
Di-calcium phosphate	1.30
DL-Methionine	0.13
Salt	0.30
Premix (Zn free)[1]	0.80
Total	100.00
Nutrient levels[2]	
Metabolizable energy (MJ/kg)	11.29
Crude protein,%	16.70
Total digestible lysine, %	0.73
Total digestible methionine, %	0.36
Total digestible methionine + cysteine, %	0.68
Calcium, %	3.39
Total phosphorus, %	0.67
Available phosphorus, %	0.34

[1]Premix provided the following per kg of the diet: Vitamin A, 10,323 IU; Vitamin D_3, 3,720 IU; Vitamin E, 37.20 mg; Vitamin K_3, 3.10 mg; thiamine, 3.10 mg; riboflavin, 8.68 mg; pyridoxine, 5.27 mg; Vitamin B_{12}, 0.026 mg; niacin, 52 mg; calcium pantothenate, 13 mg; folic acid, 2.17 mg; biotin, 0.127 mg; Fe, 112 mg; Cu, 11.2 mg; Mn, 140 mg; Se, 0.56 mg; I, 0.7 mg.

[2]Nutrient levels were calculated values.

libitum, and exposed to a 16L: 8D photoperiod. The entire experiment lasted 8 wk, including the first 2 wk of pretest, after 6 wk of formal experiment.

Sample Collection

At the end of the experiment, 2 chickens from each replicate were randomly selected and fasted for 8 h prior to slaughter. Blood was collected from the wing vein blood collection, and then slaughtered by cervical dislocation. Initially, serum samples were incubated at 37°C for 2 h, then centrifuged at 3,500 r/min at 4°C for 10 min, and the supernatant was stored at -80°C for further assay. After euthanizing, the liver and intestines were isolated. One part of the liver sample was immediately frozen in liquid nitrogen and stored at −80°C for RNA extraction and bile acid composition analysis, while another part was fixed in 4% paraformaldehyde solution for liver Lipid accumulation and histometric analysis. The anterior intestines of duodenum, jejunum and ileum were clipped with 2 to 3 cm respectively, gently cleaned with 0.9% normal saline, and then fixed in a test tube containing 4% paraformaldehyde for intestinal morphology analysis. The cecum was isolated and cut open at the end, then the contents were rapidly squeezed into a sterile cryotube with tweezers for intestinal microbiota analysis.

Antioxidant and Lipid Metabolism Indexes

The liver 10% homogenate was prepared by homogenizing 0.1 g of liver tissue with 9 mL of 0.86% normal saline. After centrifuged at 4°C at 2,500 r/min for 10 min, the supernatant was taken for correlation index determination. Antioxidant indexes mainly included copper-zinc superoxide dismutase (**CuZn-SOD**), catalase (**CAT**) and malondialdehyde (**MDA**), while lipid metabolism related indexes included triacylglycerol (**TG**), total cholesterol (**TC**), high-density lipoprotein cholesterol (**HDL-C**), low-density lipoprotein cholesterol (**LDL-C**). They were assessed using commercially available kits following the manufacturer's instructions (Nanjing Jiancheng Bioengineering Institute, China).

Morphological Analysis of Liver and Intestine

Briefly, we fixed liver and intestine samples with 4% paraformaldehyde for 48 h, dehydrated them, embedded them in paraffin, embedded them in tissue sections, and stained them with Hematoxylin and eosin. Subsequently, the liver sections were imaged using Upright Optical Microscope (Nikon Eclipse Ci-L, Japan) under a microscope through 200 x magnification. Further analysis, identification, and description were conducted on liver tissue for pathological changes, such as degeneration, inflammation, edema, and congestion. Besides, liver sections were performed using Oil red O staining to visualize lipid droplet accumulation under 400 x magnification. The percentage of lipid droplets was then analyzed by calculating the ratio of the pixel area of red to the total pixel area in each visual field using the ImageJ software. For intestinal sections, the target area was selected for 40-fold imaging after HE staining. Subsequently, the villus height and crypt depth were measured and analyzed using Image-Pro Plus 6.0 software, and finally the mean value was used as the calculated value of each sample.

Real-Time PCR for Lipid Metabolism Related mRNA Expression

Total RNA was extracted from livers using RNAiso reagent. Using a DeNovix DS-11 Spectrophotometer (DeNovix Inc.), RNA samples were quantified at 260/280 nm for concentration and purity. And then reverse transcribed to cDNA by the primescript RT reagent kit (Takara, RR037A) according to the manufacturer's instructions. Finally, qRT-PCR was performed in triplicate using HieffTM qPCR SYBR Green Master Mix kit in the ViiA7 Real-time PCR System (Thermo Fisher Scientific), according to the manufacturers instructions, and the expression of target genes was normalized to GAPDH. The sequences of PCR primers (Table 2) were synthesized by the Suzhou Jinweizhi Biotechnology Co., Ltd (Suzhou, China). We determined each target gene's relative expression using the $2^{-\Delta\Delta Ct}$ method.

Analysis of Bile Acid Compounds

The liver samples were accurately weighed at about 25 mg and transferred to EP tube. After adding 1,000 μL extract, the samples were swirled and mixed for 30 s,

Table 2. primer used for quantitative real-time PCR.

Gene	Primer sequence (5'−3')	Accession number
PPAR α	AGTAAGCTCTCAGAAACTTTGTTG GTCATTTCACTTCACGCAGCA	NM_001001464.1
SREBP 1C	ATCATGCGGCGACCGAC GCAGCATGTCGTCGATGT	NM_204126.3
ACC α	ATGGTGGGGTATGTGAGTGC CATGGCAATCTGGAGCTGTG	NM_205505.2
FAS	CCAACGATTACCCGTCTCAA CAGGCTCTGTATGCTGTCCAA	J03860
SCD	GTTCCTACTCCCCGTCACAC TCACGTAAAATACACCATGGGAGA	NM_204890.2
CYP7A1	TTCAAGAGTGCCCACAGTGC AGCATGACAAGCTCGGAGAG	NM_001001753.2
CYP27A1	ACTTTCGTCTGGCTCTTCCTG CATCGGGTATTTGCCCTCCT	XM_422056.7
SHP	GTCACCAGTAGCACGGACAT GGCTGAGGAGGGTGTAGAGA	NM_001030893
FXR	GCTCTCACTTGTGAAGGATGC GCATTTCCTTAGACGGCACTC	NM_204113.2
GAPDH	AGAACATCATCCCAGCGT AGCCTTCACTACCCTCTTG	NM_204305.2

Abbreviations: ACC α, acetyl-CoA carboxylase alpha; CYP27A1, sterol 27-hydroxylase; CYP7A1, cholesterol 7-alpha hydroxylase; FAS, fatty acid synthase; FXR, farnesoid X receptor; GAPDH, glyceraldehyde-3-phosphate dehydrogenase; PPAR α, peroxisome proliferator activated receptor alpha;

SCD, stearoyl-CoA desaturase; SHP, small heterodimer partner; SREBP 1C, sterol regulatory element binding transcription factor 1.

ground at 35 Hz for 4 min, and then transferred to ice water bath for 5 min for ultrasound, repeated 3 times. Finally, after incubation at -40°C for 1 h and centrifugation at 12,000 rpm for 15 min, the supernatant was transferred to the sample bottle for UHPLC-MS/MS analysis. Among them, the UHPLC conditions: Waters ACQUITY UPLC BEH C18 column (150 × 2.1 mm, 1.7 μm). Phase A consisted of 1 mmol/L ammonium acetate and 0.1 % acetic acid aqueous solution, and phase B consisted of acetonitrile. The temperature of the column incubator was 50°C, while the sample tray was 4°C, and the injection volume was 1 μL. The main parameters of ion source in MS: Spray voltage = +3500/-3100 V, Sheath gas (N_2) flow rate = 40, Aux gas (N_2) flow rate = 15, Sweep gas (N_2) flow rate = 0, Aux gas (N_2) temperature = 350°C, Capillary temperature = 320°C.

Sequencing and Analysis of Cecum Microorganisms

The DNA was extracted by CTAB method. After the purity of DNA were detected by 1% agarose gel electrophoresis, appropriate amount of samples were taken into a centrifuge tube and diluted to 1 ng/μL. The microorganisms were analyzed by sequencing the V_3-V_4 region of 16s RNA using upstream and downstream priors 341F (5′-CCTAYGGGRBGCASCAG-3′) and 806R (5′-GGACTACNNGGGTATCTAAT-3′), respectively. The PCR reaction program was predenaturation at 98°C for 1 min, followed by 30 cycles of 98°C for 10 s, 50°C for 30 s, and 72°C for 30 s. Subsequently, after equal concentration mixing according to the concentration of PCR products, the PCR products were purified by electrophoresis on an agarose gel with a 1×TAE concentration of 2%, and the target band was recovered by clipping. Finally, the sequencing library was constructed using Illumina's TruSeq DNA PCR-Free Sample Preparation Kit (Illumina, USA). After qualified by Qubit quantification and library detection, the constructed library was sequenced by Illumina NovaSeq 6000 (PE250).

In order to ensure the accuracy of OTU clustering and subsequent analysis, the original sequencing was first pruned, de-noised, splicing, and chimaera removed to obtain the final feature sequence. Based on this sequence, the species composition of each group was annotated and evaluated first, and the significant differences of species classification levels among groups were analyzed by LEfSe. Then, Alpha and Beta diversity analysis was performed to explore the differences in species composition between the sample groups. Finally, the sequences of measured microbial genomes were mapped to the MetaCyc database for functional predictive analysis (Langille et al., 2013; Comeau et al., 2017).

Statistical Analysis

The results were statistically analyzed by 1-way ANOVA followed by Duncan's multiple range tests (SPSS 24.0), and then regression analysis was used to test the linear and quadratic effects. Differences among treatments were deemed to be significant at $P < 0.05$, and results were presented as mean and standard error mean (**SEM**).

RESULTS

Serum Antioxidant and Lipid Metabolism Indexes

The effect of dietary PDMY-Zn NPs on serum antioxidant and lipid metabolism indexes of laying hens are listed in Table 3. There were no significant differences in CAT among the groups. The activity of CuZn-SOD in serum increase (linear and quadratic, $P < 0.05$) with increasing dietary PDMY-Zn NPs levels, whereas the amount of MDA was dramatically reduced (linear and quadratic, $P < 0.05$). Additionally, the contents of TG, TC, HDL-C, and LDL-C in serum were significantly affected by dietary PDMY-Zn NPs supplementation. The contents of TG, TC, and LDL-C in serum were decreased (linear and quadratic, $P < 0.05$). Conversely, HDL-C content was increased (linear and quadratic, $P < 0.05$) by dietary PDMY-Zn NPs levels.

Liver Antioxidant and Lipid Metabolism Related Indicators

As shown in Table 4, different levels of PDMY-Zn NPs had no significant effect on CAT activity in liver of laying hens. However, with PDMY-Zn NPs supplementation, the contents of CuZn-SOD was significantly increased linearly or quadratic, while the content of DMA was significantly decreased, and the extreme value

Table 3. Effects of PDMY-Zn NPs at different levels on serum antioxidant and lipid metabolism indexes of laying hens.

Items	PDMY-Zn NPs levels (mg/kg)				SEM	*P-value*		
	T0	T200	T400	T600		ANOVA	Linear	Quadratic
CuZn-SOD (U/mL)	75.84[a]	79.64[ab]	81.38[b]	83.52[b]	0.85	0.004	<0.001	0.001
CAT (U/mL)	4.73	4.86	4.88	4.92	0.20	0.991	0.757	0.949
MDA (nmol/mL)	10.52[a]	9.64[ab]	8.51[c]	9.13[bc]	0.22	0.004	0.005	0.002
TG (mmol/L)	20.90[a]	18.19[ab]	14.44[c]	14.79[bc]	0.78	0.003	<0.001	0.001
TC (mmol/L)	5.47[a]	5.00[a]	3.70[b]	3.76[b]	0.24	0.008	0.001	0.005
HDL-C (mmol/L)	0.81[b]	0.87[ab]	1.01[a]	0.98[a]	0.03	0.049	0.011	0.029
LDL-C (mmol/L)	0.48[a]	0.36[b]	0.33[b]	0.32[b]	0.02	0.002	0.001	0.001

Abbreviations: CAT, catalase; CuZn-SOD, copper-zinc superoxide dismutase; HDL-C, high-density lipoprotein cholesterol; LDL-C, low-density lipoprotein cholesterol; MDA, malondialdehyde; TC, total cholesterol; TG, triacylglycerol.
[a,b,c]Values without the same letters within the same line indicate a significant difference ($P < 0.05$).

Table 4. Effects of PDMY-Zn NPs at different levels on antioxidant and lipid metabolism indexes in liver of hens.

Items	PDMY-Zn NPs levels (mg/kg)				SEM	*P-value*		
	T0	T200	T400	T600		ANOVA	Linear	Quadratic
CuZn-SOD (U/mgprot)	42.82[b]	48.85[a]	50.44[a]	50.42[a]	1.15	0.046	0.014	0.018
CAT (U/mgprot)	9.07	9.86	10.52	10.31	0.37	0.547	0.192	0.345
MDA (nmol/mgprot)	6.33[a]	5.30[b]	4.64[b]	4.80[b]	0.19	0.004	0.001	0.001
TG (mmol/L)	0.85	0.80	0.83	0.73	0.03	0.306	0.137	0.279
T-C (mmol/L)	0.43[a]	0.36[ab]	0.31[b]	0.33[b]	0.02	0.034	0.011	0.013
HDL-C (mmol/L)	0.16[b]	0.33[a]	0.33[a]	0.34[a]	0.02	0.001	<0.001	<0.001
LDL-C (mmol/L)	0.047[a]	0.049[a]	0.037[b]	0.036[b]	0.01	0.005	0.002	0.008

Abbreviations: CAT, catalase; CuZn-SOD, copper-zinc superoxide dismutase; HDL-C, high-density lipoprotein cholesterol; LDL-C, low-density lipoprotein cholesterol; MDA, malondialdehyde; TC, total cholesterol; TG, triacylglycerol.
[a,b]Values without the same letters within the same line indicate a significant difference ($P < 0.05$).

appeared in 400 mg/kg group ($P < 0.05$). Similarly, the contents of TC and LDL-C in liver were significantly decreased (linear and quadratic, $P < 0.05$) with PDMY-Zn NPs supplementation, while the content of HDL-C was significantly increased (linear and quadratic, $P < 0.05$). In addition, the content of TG in liver also decreased, but did not reach a significant level.

Liver Morphology and Lipid Droplet Content

The effect of dietary PDMY-Zn NPs on the liver morphology of laying hens was listed in Figure 1. In the control group, vacuolar degeneration of hepatocytes was more common, and a large focal infiltration of inflammatory cells was seen around the blood vessels (Figure 1A). The 200 mg/kg of PDM-Zn NPs group was similar to

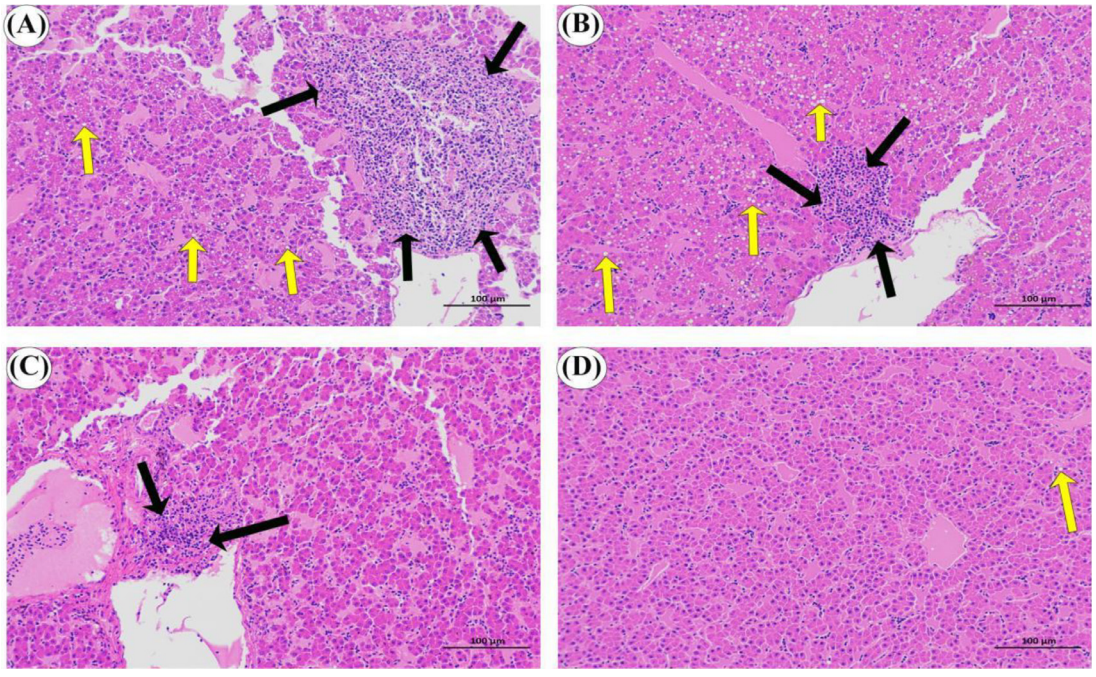

Figure 1. Effects of PDMY-Zn NPs at different levels on liver lipid droplet content of laying hens. (A) T0, (B) T200, (C)T400, (D) T600. The yellow arrows in the figure point to the hepatocyte cytoplasm vacuoles, and the black arrows point to the focal infiltration of inflammatory cells.

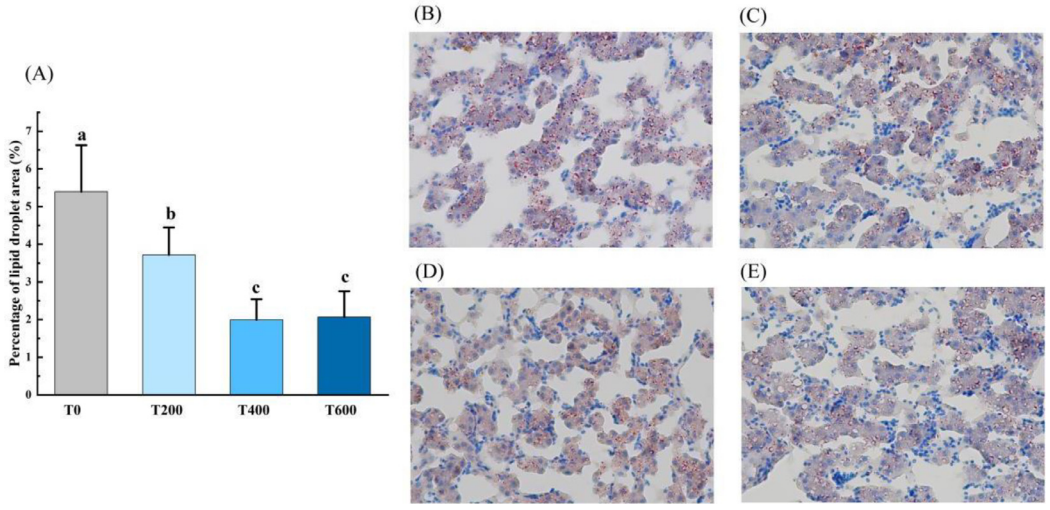

Figure 2. Effects of PDMY-Zn NPs at different levels on liver lipid droplet content of laying hens. (A) The percentage of lipid droplet surface area(400 magnification); (B) T0, (C) T200, (D)T400, (E) T600. [a,b,c] Values without the same letters within the same line indicate a significant difference ($P < 0.05$).

the control group in vacuolar degeneration of hepatocytes, but the focal infiltration of inflammatory cells around the blood vessels was alleviated (Figure 1B). The liver cells were equally pigmented, the cytoplasm was abundant, and there was no evident vacuolar degeneration in the 400 mg/kg PDM-Zn NPs group. Instead, a small number of inflammatory cells infiltrated (Figure 1C). Regarding 600 mg/kg PDM-Zn NPs, less vacuolar degeneration and no obvious necrosis or inflammatory reaction was found in the tissue (Figure 1D). Overall, the outcome exhibited that the supplementation of PDMY-Zn NPs in hens diet can reduce the vacuolar degeneration of hepatocytes and prevent or treat the inflammatory response of hepatocytes.

Figure 2 illustrates the effect of dietary PDMY-Zn NPs on the content of lipid droplets in laying hens. The number of red pixels, which indicate the buildup of lipid droplets, reduced in each segment as dietary PDM-Zn NPs content increased. Furthermore, the lowest accumulation of liver lipid droplet was noted in 400 and 600 mg/kg PDM-Zn NPs as compared to control and 200 mg/kg PDM-Zn NPs.

Relative Expression of Lipid Metabolism-Related Genes

The effect of dietary PDMY-Zn NPs on the relative expression of lipid metabolism-related genes of laying hens was listed in Figure 3. FAS and CYP27A1 mRNA levels in the liver did not significantly differ between the groups. As the concentration of PDMY-Zn NPs increased in the diet, the relative expression level of PPAR α, FXR and SHP were noticeably up-regulated in comparison to the control, with the highest values in the 400 mg/kg group ($P < 0.05$). However, a significant decreasing trend was exhibited for ACC α and SCD mRNA ($P < 0.05$), particularly in the 400 mg/kg group. Similarly, SREBP 1C and CYP7A1 mRNA were also down-regulated in the PDMY-Zn NPs diet compared to the control ($P < 0.05$).

Intestinal Mucosa Morphology

As shown in Table 5, dietary supplementation with different levels of PDMY-Zn NPs had no significant effects on jejunum villus height, crypt depth, and villus/crypt (**V/C**) ratio. However, the villus height and V/C of duodenum were significantly increased with PDMY-Zn NPs supplementation ($P < 0.01$). Similarly, the villus height and V/C of the ileum also showed linear or quadratic increases ($P < 0.05$), while the crypt depth of the duodenum and ileum was less affected by PDMY-Zn NPs supplemental level.

Composition and Abundance of Cecal Microorganisms

The composition and abundance analysis of cecal microorganisms of laying hens was shown in Figure 4. With the increase of dietary PDMY-Zn NPs, the OTU of each group showed a gradual downward trend. There were 826 OTUs in common among all treatment groups, of which 355 were in T0 and T200 groups, followed by 130 in T400 and T600 groups (Figure 4C). At the phylum level (Figure 4A), *Bacteroidetes, Firmicutes, Proteobacteria*, and *Fusobacteria* were the dominant microorganisms. Among them, the abundance of *Bacteroidetes* and *Firmicutes* in all groups exceeded 80%, and the ratio of F/B between all groups was different. Compared with T0 group, the F/B value in 200 mg/kg and 600 mg/kg groups was decreased, while that in 400 mg/kg group was increased, but no significant difference was reached. At the genus level (Figure 4B), the microorganisms were composed of *Bacteroides, Unspecified Bacteroidales, Ruminococcus, Unspecified Ruminococcaceae, Desulfovibrio* and other microorganisms. With the increase of PDMY-Zn NPs, *Bacteroides*

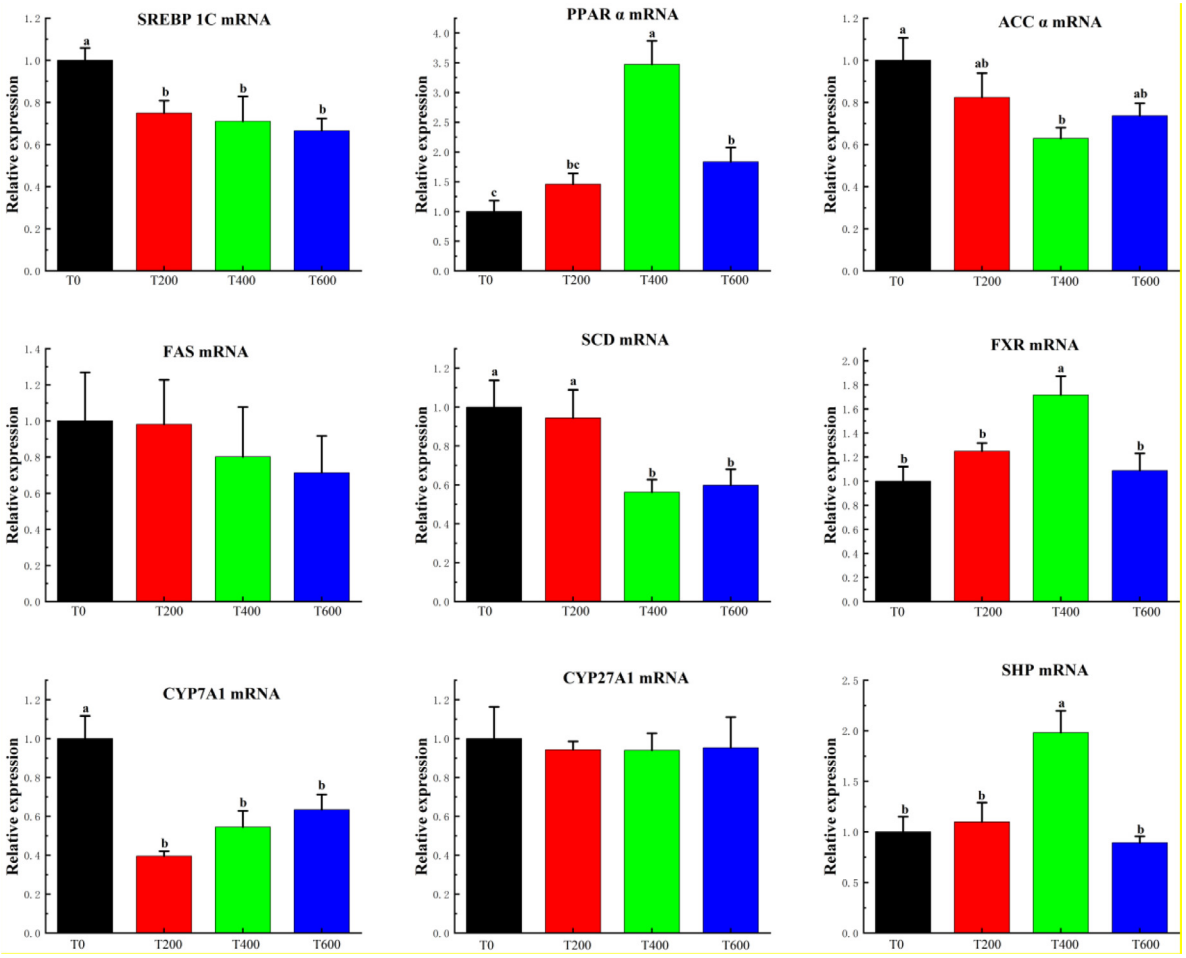

Figure 3. Effects of PDMY-Zn NPs at different levels on relative expression of lipid metabolism-related genes of laying hens. SREBP 1C = sterol regulatory element binding transcription factor 1, PPAR α = peroxisome proliferator activated receptor alpha, ACC α = acetyl-CoA carboxylase alpha, FAS = fatty acid synthase, SCD = stearoyl-CoA desaturase, FXR = farnesoid X receptor, CYP7A1 = cholesterol 7-alpha hydroxylase, CYP27A1 = sterol 27-hydroxylase, SHP = small heterodimer partner. [a,b,c] Values without the same letters within the same line indicate a significant difference (P <0.05).

showed a gradual increasing trend. To obtain the characteristic microorganisms of each treatment group, the difference of flora abundance at the genus level between groups was tested by LEfSe method (Figure 4D). In other words, there was a higher abundance of microbes in this group relative to the other groups ($P < 0.05$). The characteristic microorganisms of T0 treatment group were *f_ Clostridiaceae, g_ Clostridium, etc.* The characteristic microorganisms of T200 group were *f_ Prevotellaceae, g_ Prevotella, etc.* The characteristic microorganisms in T400 group were *f_ Lactobacillaceae, g_ Lactobacillus, etc.* The characteristic microorganisms of T600 group were *k_ Bacteria, g_ Megamonas, etc.*

Table 5. Effects of PDMY-Zn NPs at different levels on intestinal mucosal morphology of laying hens.

	PDMY-Zn NPs levels (mg/kg)					*P-value*		
Items	T0	T200	T400	T600	SEM	ANOVA	Linear	Quadratic
Duodenum								
V(μm)	968.68[b]	1374.74[a]	1509.04[a]	1412.39[a]	56.33	<0.001	0.002	<0.001
C (μm)	48.75	40.67	46.25	42.65	1.80	0.408	0.441	0.622
V/C	20.23[b]	35.11[a]	33.48[a]	34.21[a]	1.87	0.005	0.012	0.004
Jejunum								
V (μm)	899.69	855.13	988.14	1063.37	41.28	0.297	0.091	0.188
C(μm)	45.00	36.47	34.59	40.24	2.26	0.396	0.436	0.218
V/C	19.90	24.30	28.99	29.42	1.51	0.072	0.010	0.030
Ileum								
V (μm)	602.56[c]	751.74[b]	914.35[a]	898.72[a]	34.23	<0.001	<0.001	<0.001
C (μm)	31.65	36.86	34.98	35.07	1.09	0.417	0.403	0.363
V/C	19.73[b]	20.73[b]	26.14[a]	25.89[a]	1.01	0.026	0.005	0.020

Abbreviations: C, crypt depth; V, villus height; V/C, villus height/crypt depth.
[a,b,c]Values without the same letters within the same line indicate a significant difference ($P < 0.05$).

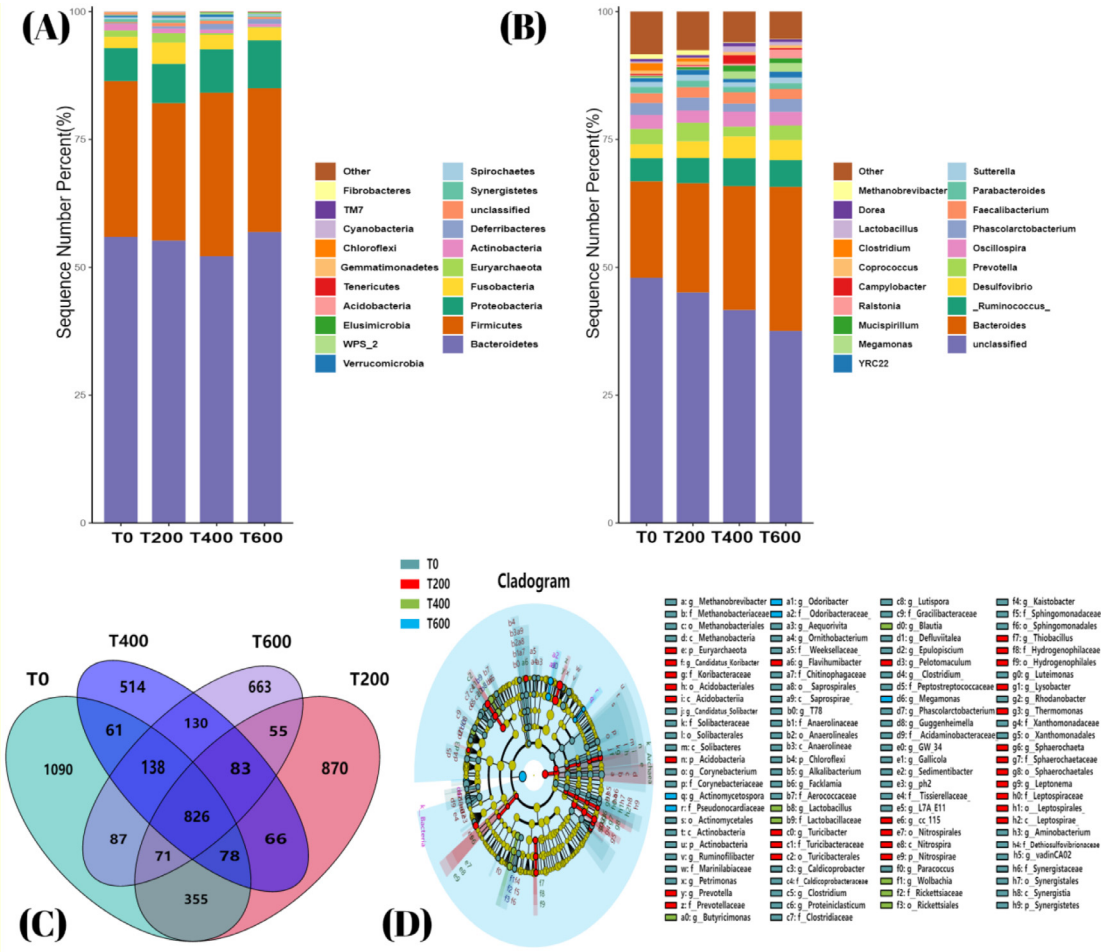

Figure 4. Effects of PDMY-Zn NPs at different levels on composition and abundance of caecum microorganisms in laying hens. (A) Microbial composition at phylum level, (B) Microbial composition at genus level, (C) Venn diagram, (D) LEfSe analysis of cladogram

Microbial Diversity Analysis and Prediction Functions

Alpha diversity index commonly used in the analysis of species diversity in samples, usually including OTU, Chao1, Shannon and Simpson index. As shown in Figure 5A, the OTU, Chao1 and Shannon indices of cecal microflora of laying hens decreased with the increase of PDMY-Zn NPs supplementation, but there were no significant differences among all groups. Beta diversity used to compare the composition of microbial communities among different samples. In this study, PERMANOVA and ANOSIM methods were used to compare whether there were significant differences among experimental groups. As shown in Figure 5B, The Beta diversity of the T0 and T200 treatment groups was similar, but both were significantly different from the T400 group. Similar results also existed in the T600 group, but there was no significant difference from the T400 group. Based on MetaCyc database, a total of 407 bacteria-related metabolic pathways were predicted in this study (Figure 5C). Among them, The most abundant pathways were gondoate biosynthesis (PWY-7663), pentose phosphate pathway I (NONOXIPENT-PWY), L-isoleucine biosynthesis II (PWY-5101), cis-vaccenate biosynthesis (PWY-5973), pyruvate fermentation to isobutanol (PWY-7111), and quercetin glucoside biosynthesis (PWY-7129), superpathway of pyrimidine nucleobases salvage (PWY-7208), L-isoleucine biosynthesis IV (PWY-5104), glycolysis III (ANAGLYCOLYSIS-PWY), *etc.* The ANOVA+Duncan method was used to analyze the significant difference of microbial community prediction function between groups. As shown in Figure 5C, the abundance of superpathway of *Kdo2-lipid A* biosynthesis (LPSSYN-PWY) increased with the increase of PDMY-Zn NPs, and the highest value appeared in the T600 group ($P < 0.05$). Meanwhile, the relative abundances of NAD *de novo* biosynthesis II (NADSYN-PWY), L-tryptophan degradation IX (PWY-5655), formaldehyde assimilation I (PWY-1622), glycogen degradation II (PWY-5941) pathways were similar in the T0 and T200 treatment groups, but significantly decreased in the T400 and T600 groups ($P < 0.05$).

Bile Acid Compounds in Liver

The effect of dietary PDMY-Zn NPs on Bile acid compounds (BAs) in liver of laying hens was listed in Figure 6. With the increase of PDMY-Zn NPs supplementation, the composition of BAs in liver of each group

(A)

Items	OTU	Chao1	Shannon	Simpson
T0	934.13	929.83	8.14	0.988
T200	867.36	864.83	8.14	0.990
T400	781.68	779.17	7.90	0.988
T600	800.23	798.33	7.86	0.989
SEM	34.34	34.42	0.07	0.01
P-value	0.415	0.405	0.342	0.941

(B)

Items		ANOSIM analysis			PERMANOVA analysis		
		R	*P*-value	q-value	pseudo-F	*P*-value	q-value
T0	T200	-0.137	0.993	0.993	0.700	0.989	0.989
	T400	0.231	0.009	0.015	1.689	0.006	0.009
	T600	0.270	0.002	0.012	1.920	0.006	0.009
T200	T400	0.256	0.010	0.015	1.649	0.002	0.009
	T600	0.261	0.005	0.015	1.837	0.004	0.009
T400	T600	-0.048	0.602	0.722	0.937	0.511	0.613

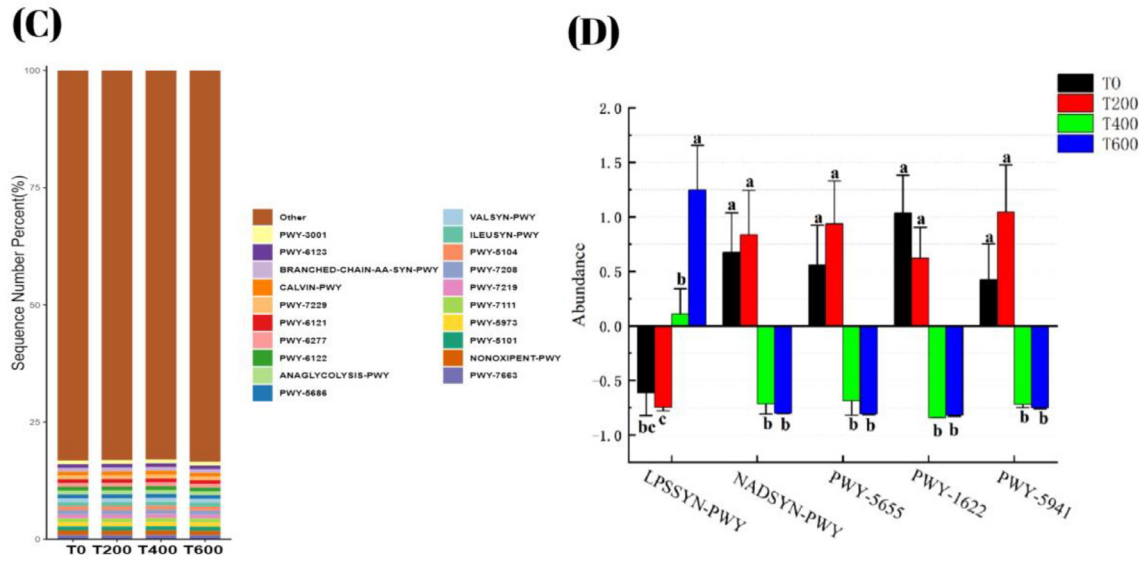

Figure 5. Effects of PDMY-Zn NPs at different levels on Microbial diversity analysis and prediction functions in laying hens. (A) Alpha diversity analysis, (B) Beta diversity analysis, (C) MetaCyc pathway prediction diagram, (D) MetaCyc pathways significant analysis. [a,b,c] Values without the same letters within the same line indicate a significant difference ($P < 0.05$).

showed different degrees of upward trend. The total BAs increased first and then decreased, and the maximum value was found in T400 treatment group ($P < 0.05$). Interestingly, similar results were found for primary BAs and secondary BAs ($P < 0.05$). The unconjugated BAs in T200 and T600 treatment groups were higher than in T0 and T400 groups, but conjugated BAs in T400 treatment group were significantly higher than other

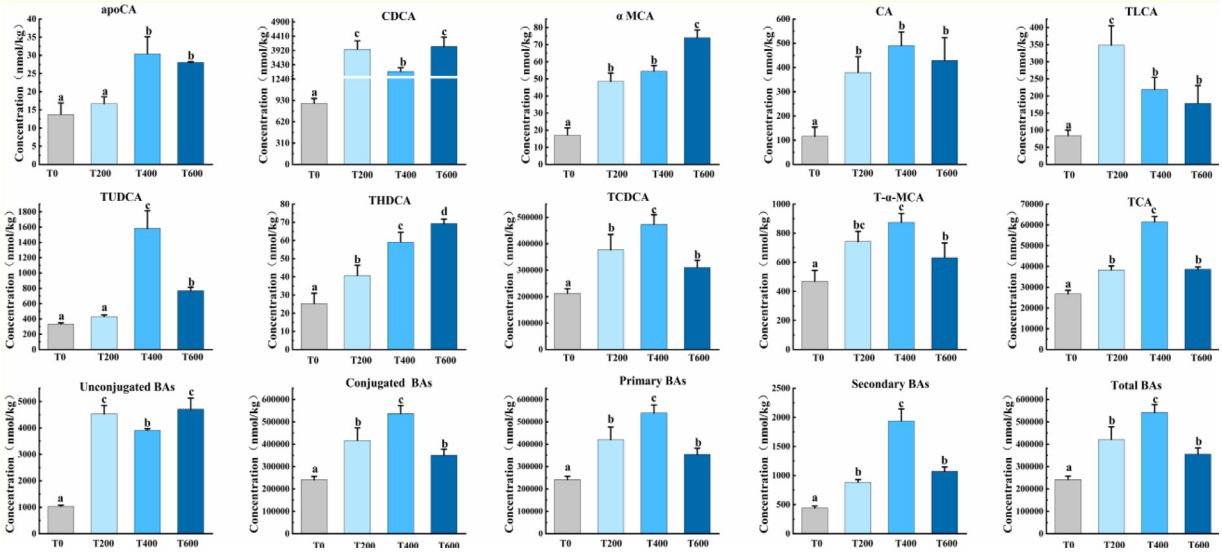

Figure 6. Effects of PDMY-Zn NPs at different levels on BAs in liver of laying hens. apoCA = Apocholic acid, CDCA = Chenodeoxycholic acid, α MCA = α-Muricholic acid, CA = Cholic acid, TLCA = Taurolithocholic acid, TUDCA = Tauroursodeoxycholic acid, THDCA = Taurohyodeoxycholic acid, TCDCA = Taurochenodeoxycholic acid, T-α-MCA = Tauro α-Muricholic acid, TCA = Taurocholic acid. [a, b,c,d] Values without the same letters within the same line indicate a significant differe nce ($P < 0.05$).

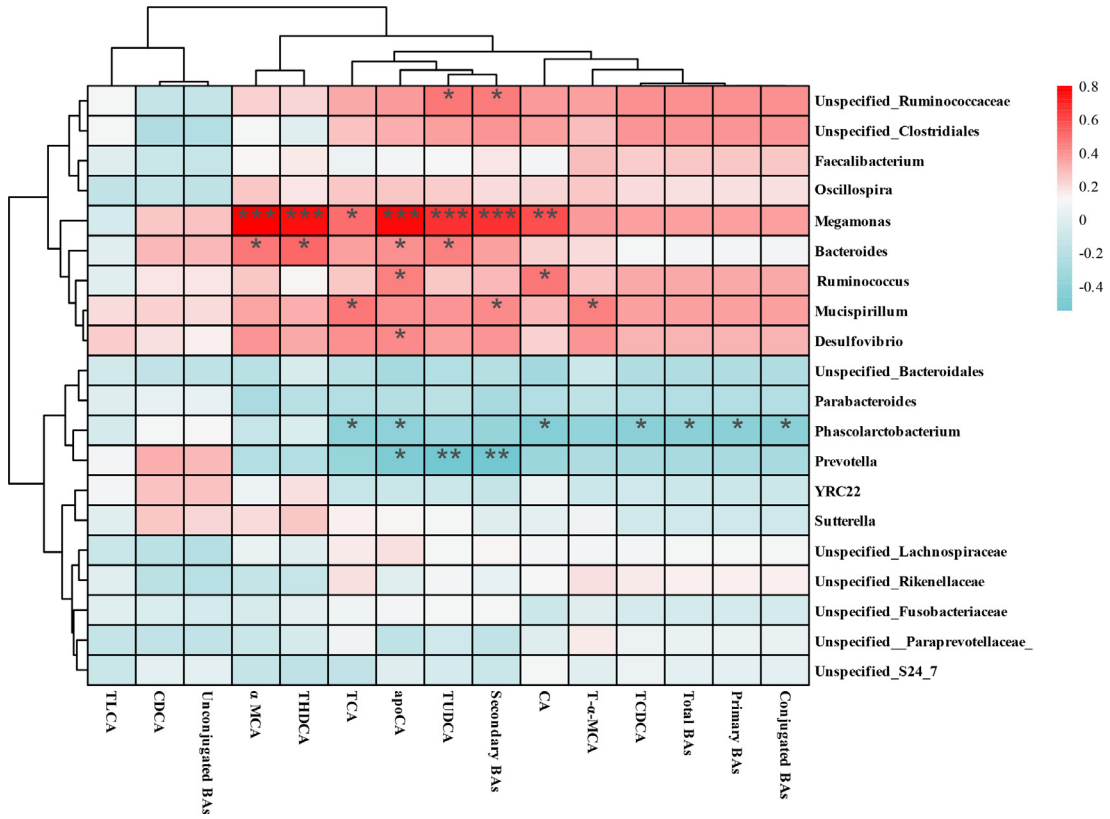

Figure 7. The relationship between the changes of intestinal flora structure and the metabolism of BAs. apoCA = Apocholic acid, CDCA = Chenodeoxycholic acid, α MCA = α-Muricholic acid, CA = Cholic acid, TLCA = Taurolithocholic acid, TUDCA = Tauroursodeoxycholic acid, THDCA = Taurohyodeoxycholic acid, TCDCA = Taurochenodeoxycholic acid, T-α-MCA = Tauro α-Muricholic acid, TCA = Taurocholic acid. *$P \leq 0.05$, **$P \leq 0.01$, ***$P \leq 0.001$

treatment groups ($P < 0.05$). Compared to the T0 control group, Dietary supplementation with PDMY-Zn NPs significantly increased the contents of chenodexycholic aid (CDCA), α-Muricholic acid (**α MCA**), Taurolithocholic acid (**TLCA**), Taurohyodeoxycholic acid (**THDCA**) in liver of laying hens ($P < 0.05$). After the increase of PDMY-Zn NPs, there was a general trend of decline in the content of apocholic acid (**apoCA**), tauroursodeoxycholic acid (**TUDCA**), taurochenodeoxycholic acid (**TCDCA**), tauro alpha Muricholic acid (**T-α-MCA**), and taurocholic acid (**TCA**) after an initial rise. Among them, TUDCA, TCDCA and TCA reached their maximum values in the T400 group ($P < 0.05$).

The relationship between the changes of intestinal flora structure and the metabolism of BAs was listed in Figure 7. The majority of BAs were positively correlated with *Megamonas, Bacteroides, Mucispirillum*, while negatively correlated with *Phascolarctobacterium* and *Prevotella. Megamonas* exhibited a positive correlation with α MCA, THDCA, apoCA, TUDCA, CA, and secondary BAs ($P \leq 0.01$). Similarly, *Bacteroides* demonstrated a significant positive correlation with α MCA, THDCA, apoCA, and TUDCA ($P \leq 0.05$). There was a significant positive association between *Mucispirillum* and TCA, secondary BAs, and T-α-MCA ($P \leq 0.05$). Nevertheless, *Phascolarctobacterium* was significantly negatively associated with TCA, apoCA, CA, TCDCA, primary BAs, secondary BAs, and total BAs ($P \leq 0.05$). Meanwhile, *Prevotella* was significantly negatively correlated with apoCA, TUDCA, and secondary BAs ($P \leq 0.05$).

DISCUSSION

Oxidative stress occurs when the production of oxidants exceeds the ability of antioxidants to degrade (Forman et al., 2021). It is a component of many diseases and contributes to the occurrence and progression of liver damage (Li et al., 2015). Recently, a large number of natural plants have been applied as antioxidants to eliminate alcohol-induced liver damage, in which the bioactive ingredients responsible for alleviating oxidative stress are often attributed to polyphenols and flavonoids (Zhou et al., 2022; Jin et al., 2020; Li et al., 2021). DMY is an important natural flavonoid, and as a potential chronic disease prevention antioxidant, its biological activity has been extensively evaluated through multiple cellular and animal models (Chen et al., 2021b). Guo et al.(2021) showed that dietary supplementation of 300 and 500 mg/kg increased serum total superoxide dismutase level, serum and liver reduced glutathione, muscle CAT and serum HDL-C level, while decreased liver MDA and muscle TG level in finishing pigs. Our study demonstrated that dietary supplementation of PDMY-Zn NPs led to both linear and quadratic reductions in DMA, TC, and LDL-C levels in the serum and liver of laying hens. Conversely, there were linear and quadratic

increases in CuZn-SOD and HDL-C contents, with the most significant changes observed in the 400 mg/kg group. Similarly, the supplementation of DMY has been shown to enhance lipid metabolism and antioxidant capacity in various animal models, including mice (Guo et al., 2022), shrimp (Lu et al., 2023), Hybrid Grouper (Wang et al., 2022), and broiler chicks (Shi et al., 2022).

As an important part of lipid synthesis and metabolism regulation in laying hens, the liver is easily disturbed by factors such as diet composition, oxidative stress, hormone level, and cage feeding, which can easily lead to lipid metabolism disorder (Gao et al., 2019). The main symptoms are massive deposition of tissue fat, inflammation, and increased lipid droplets, which seriously damage the production performance and egg quality of laying hens (Shini et al., 2019). Numerous studies have demonstrated that the condition of adipose tissue in obesity and other pathologies is closely related to Zn status (Olechnowicz et al., 2018). Qi et al. (2020) discovered that high doses of zinc can alleviate glucose and lipid metabolism disorders caused by nonalcoholic fatty liver disease by reducing glucose production, promoting body absorption, and decreasing lipid deposition. Furthermore, Zhao et al. (2016) proposed that ZnO NP influenced egg quality and specifically regulated lipid metabolism in hens by altering the function of the hen's ovary and liver. Zhang et al. (2018) also identified that ZnO NPs disrupted lipid metabolism in the liver and thereby affected blood lipid balance in laying hens. Interestingly, Chi et al. (2023) developed a novel zinc supplement (UO-Zn) using ulvan oligosaccharide (**UO**) as a ligand and found that it significantly decreased body and adipose tissue weight by enhancing the reverse of cholesterol transport and fatty acid β-oxidation. It is hypothesized that UO serves as a functional ligand and works synergistically with Zn to enhance lipid metabolism. Similarly, Wassie et al. (2022) found that Enteromorpha polysaccharide-Zn promotes fatty acid oxidation and inhibits fat synthesis in chickens by modulating the expression of lipid metabolism-related genes. In this study, it was found that there were much mild vacuolar degenerations of hepatocytes in liver morphology of control group, small vacuoles were observed in the cytoplasm, and several inflammatory cell focal infiltrations were observed around the blood vessels, which were suspected to have mild FLHS symptoms. With the addition of dietary PDMY-Zn NPs, the vacuolar degeneration and inflammatory necrosis of hepatocytes decreased. Moreover, the content of lipid droplets in liver also decreased, indicating that PDMY-Zn NPs can alleviate the further deterioration of FLHS in laying hens. Zeng et al. (2020) also found that adding DMY to high fat diet alleviated metabolic disorders and improved liver histopathology in mice, including liver steatosis, inflammation, and fibrosis. Song et al. (2022) found that DMY can improve the deposition of lipid droplets in the liver of leptin-deficient mice. Similar studies have also shown that DMY can reduce liver injury caused by lipopolysaccharide (Shi et al., 2022). This might be associated with the augmentation of Zn supplementation, and is more prone to be related to the hypoglycemic and hypolipidemic activities of its ligand DMY (Liu et al., 2019). Simultaneously, it could also be attributed to the synergy of DMY and Zn, and even give rise to novel pharmacological activities, which requires further study.

The liver is the primary organ to encounter microbial products that traverse the intestinal epithelial barrier, and homeostasis is influenced by the composition of gut microbiota and bacterial metabolites (Trebicka et al., 2021). Dysregulation of intestinal microorganisms and increased intestinal permeability are linked to the pathogenesis of numerous CLD (Xu et al., 2022). Hamid et al. (2019) utilized laying hens as an experimental model to investigate the correlation between cecal flora and nonalcoholic steatohepatitis (**NASH**). And findings indicated that dysbiosis of cecal microbiota was associated with the severity of fibrosis and NASH at various stages. The cecum is the site of highest microbial density and diversity in the intestinal tract of laying hens, with *Firmiculus* as the predominant group, followed by *Bacteroides* (Bindari et al., 2022). Changes in the relative abundance and ratio of *Firmiculus* and *Bacteroides* are important indicators reflecting the balance of intestinal microflora, and closely related to obesity, diarrhea and other diseases (Turnbaugh et al., 2006). Our results also indicated that *Firmicutes* and *Bacteroidetes* were dominant in the cecum of laying hens, accounting for over 80% of flora abundance. Among them, *Firmicutes* and F/B values were reduced in the 200 mg/kg and 600 mg/kg groups. with the increase of dietary PDMY-Zn NPs level, the alpha diversity index of OTU, Chao1, Shannon and Simpson of cecal flora showed a downward trend. Similar studies showed that dietary DMY supplementation significantly reduced the diversity of OTU and alpha in mice gut microbes, and increased *Bacteroides*, while *Firmicutes* and F/B values significantly decreased (Fan et al., 2018). Additionally, the current study also identified significant variances in the characteristic microorganisms at the genus level among the groups. The control group was distinguished by *Clostridium*, while the cecum microflora of laying hens was characterized by *Lactobacillus, Prevotella and Macroomonas* with PDMY-Zn NPs supplementation. Dong et al. (2019) research also demonstrated that dietary supplementation of DMY significantly elevated levels of intestinal *Lactobacillus* and *Akkermansia* in mice. *Lactobacillus*, as a probiotic, plays a crucial role in maintaining intestinal health. It can produce Short-chain fatty acid (**SCFA**), lactic acid, hydrogen peroxide, bactericin and other antibacterial substances through metabolic decomposition (Khan et al., 2020), or competitively inhibit pathogen adhesion to intestinal epithelial sites (Collado et al., 2007). *Prevotella* is a gram-negative anaerobic bacterium with immune modifying properties and inhibition of inflammatory cytokines. It ferments dietary fiber to produce SCFA acetate (Franke et al., 2018), which has potent anti-inflammatory effects partly by promoting IL-10 production for T cell regulation (Furusawa et al., 2013) and stimulating innate immune cell development through succinic acid production from dietary fiber and fat metabolism (Rubic et al., 2008).

Macroomonas can generate metabolites such as acetic acid, propionic acid and lactic acid through carbohydrate fermentation to further contribute to bodily material metabolism or immune regulation functions for intestinal health (Rauf et al., 2022) In conclusion, this study demonstrated that PDMY-Zn NPs alters the composition and diversity of microbes in the cecum tract and enhances the abundance of probiotics, which may contribute to alleviating liver lipid metabolism disorders in laying hens. Another study also indicated that DMY mitigated nonalcoholic steatohepatitis in mice by upregulating gut probiotics and inhibiting harmful gut bacteria (Miao et al., 2023).

BAs are crucial metabolites in the intestine, categorized into primary bile acids synthesized directly from cholesterol in the liver, and secondary bile acids excreted into the intestine and then dehydroxylated by intestinal bacteria (Kobayashi et al., 2022). In order to gain a deeper understanding of the impact of PDMY-Zn NPs on lipid metabolism in the livers through the regulation of intestinal microorganisms, we conducted analyses on bile acid metabolism levels and mRNA expression of key regulatory factors in the liver of laying hens using UHPLC-MS/MS and qPCR. The study revealed that dietary supplementation of PDMY-Zn NPs generally led to an increase in the concentration of bile acids in the liver. Specifically, the levels of primary bile acids, secondary bile acids, and total bile acids initially increased and then decreased in response to the increasing supplemental level of PDMY-Zn NPs, and maximum values occurred in the 400 mg/kg group. Bile acids prevent overgrowth of gut bacteria and exert a powerful antibacterial effect on gut homeostasis (Kurdi et al., 2006). This may be an important reason for the decreased microbial diversity in the cecum of laying hens in experimental group. Further, BAs synthesis is the main pathway of cholesterol metabolism, and it also serves as a variety of functional signaling factors, mainly involved in regulating lipid, glucose, and energy metabolism through nuclear receptors and related signaling pathways, thus playing an important physiological role in regulating lipid homeosta (Chiang et al., 2009). The synthesis of BAs primarily involves the classical pathway as the main route, with CYP7A1 serving as the key rate-limiting enzyme. The alternative pathway mainly operates under pathological conditions in the body, where CYP27A1 acts as the key rate-limiting enzyme (Russell et al., 2003). BAs regulate their own synthesis, metabolism, and homeostasis by modulating FXR and related pathways (Matsubara et al., 2013). FXR can induce SHP in a dependent manner to inhibit CYP7A1 expression (Chiang et al., 2009). Additionally, BAs can mediate FXR to induce PPARα expression for suppressing nuclear receptor 4α activity in hepatocytes and inhibiting CYP7A1 transcription. Moreover, PPARα also regulates CYP27A1 expression in macrophages (Pineda et al., 2003). Interestingly, this study demonstrated that dietary supplementation of 400 mg/kg PDMY-Zn NPs up-regulated the relative expression levels of FXR and SHP in liver, down-regulated CYP7A1, but had no significant effect on CYP27A1. Collectively, the present study indicated that PDMY-Zn NPs may enhance BAs synthesis through a classical pathway, and the synthesized BAs can inhibit the relative expression of CYP7A1 through FXR-dependent mediating SHP or inducing PPARα expression after the hepato-intestinal cycle, thus maintaining the metabolic balance of BAs.

Lipid deposition largely depends on the balance between body lipid synthesis and lipolysis, which is regulated by a large number of related enzymes, key genes, and signaling pathways (Emami et al., 2020). Currently, the exact regulatory mechanism of PDMY-Zn NPs on lipid metabolism has not been elucidated. Recent studies have generally recognized that DMY primarily regulates lipid metabolism through 2 main mechanisms (Chen et al., 2021a). Firstly, DMY activates the expression of AMPK and its target genes to inhibit fatty acid synthesis and promote fatty acid β-oxidation, thereby mitigating hepatic steatosis. Additionally, DMY suppresses the production of reactive oxygen species by upregulating the expression of Nuclear erythroid 2-related factor 2 and its antioxidant products, thus ameliorating oxidative stress. ACC and FAS are key rate-limiting enzymes in de novo lipogenesis, which are regulated by LXRα, PPAR and SREBP 1c (Song et al., 2018). Besides, ACC and FAS are target genes of SREBP 1c, which promote fat biosynthesis by directly promoting their expression (Horton et al., 2002). LXRα is a ligand-activated nuclear receptor that promotes the expression of SREBP 1c and activates ACC and FAS, while PPARα plays an important role in regulating fat β-oxidation (Wang et al., 2020). A dietary DMY supplementation reduces lipid accumulation in finishing pigs through activation of AMPK/ACC signaling and regulation mRNA expression of genes related to lipogenesis, lipolysis and fatty acid oxidation, according to Guo et al. (2021). Similar studies have also shown that DMY can inhibit liver lipid de novo synthesis by down-regulating the relative expression of SREBP-1c/FAS (Song et al., 2022). We indicated that dietary supplementation of 400 mg/kg PDMY-Zn NPs significantly up-regulated the relative expression of PPARα in liver, while the relative expression of SREBP 1C, ACC, FAS and SCD was significantly down-regulated. Accordingly, the present study hypothesized that PDMY-Zn NPs may be involved in the regulation of key enzyme activity or key gene expression in the process of lipid synthesis and lipoclasis to regulate lipid metabolism in laying hens, but the specific way of regulation still needs further study.

CONCLUSIONS

This study demonstrates that the dietary supplementation of PDMY-Zn NPs can enhance the antioxidant

capacity of blood and liver in laying hens. Additionally, it reduces vacuolar degeneration and inflammatory necrosis of liver cells, decreases the content of liver lipid droplets, improves the relative expression levels of lipid metabolism-related parameters and key regulatory genes. It also remodels the composition and diversity of cecum microorganisms, increases the abundance of beneficial probiotics such as *Lactobacillus* and *Prevotella*, enhances villus height and villus/crypt ratio in the duodenum and ileum to maintain intestinal mucosal integrity. Furthermore, it increases BAs content and relative expression of key genes involved in liver synthesis. These changes may help alleviate hepatic lipid metabolism disorder in laying hens by mediating hepatoenteric circulation of BAs to improve FLHS. This study has important implications for developing flavonoids related to PDMY-Zn NPs structure, providing a theoretical basis for their development as functional feed additives for daily life and clinical prevention of CLD.

ACKNOWLEDGMENTS

This work was supported by the Guangzhou science and technology plan projects (202206010035), Qingyuan science and technology plan projects (2022KJJH068), Hainan Provincial Natural Science Foundation of China (324QN300). Agricultural Product Quality and Safety Project of Ministry of Agriculture and Rural Affairs of China (08240054)

DISCLOSURES

We declare that we have no financial and personal relationships with other people or organizations that can inappropriately influence our work, and there is no professional or other personal interest of any nature or kind in any product, service and/or company that could be construed as influencing the content of this paper.

SUPPLEMENTARY MATERIALS

Supplementary material associated with this article can be found in the online version at doi:10.1016/j.psj.2024.104301.

REFERENCES

Abd El-Hack, M. E., M. Alagawany, M. Arif, M. T. Chaudhry, M. Emam, and A. Patra. 2017. Organic or inorganic zinc in poultry nutrition: A review. World's Poult. Sci. J. 73:904–915.

Allameh, A., R. Niayesh-Mehr, A. Aliarab, G. Sebastiani, and K. Pantopoulos. 2023. Oxidative stress in liver pathophysiology and disease. Antioxidants 12:1653.

Arroyave-Ospina, J. C., Z. Wu, Y. Geng, and H. Moshage. 2021. Role of oxidative stress in the pathogenesis of non-alcoholic fatty liver disease: Implications for prevention and therapy. Antioxidants 10:174.

Bindari, Y. R., and PF. Gerber. 2022. Centennial Review: Factors affecting the chicken gastrointestinal microbial composition and their association with gut health and productive performance. Poult. Sci 101:101612.

Chen, J., X. Wang, T. Xia, Y. Bi, B. Liu, J. Fu, and R. Zhu. 2021a. Molecular mechanisms and therapeutic implications of dihydromyricetin in liver disease. Biomed. Pharmacother 142:111927.

Chen, L., M. Shi, C. Lv, Y. Song, Y. Wu, S. Liu, Z. Zheng, X. Lu, and S. Qin. 2021b. Dihydromyricetin acts as a potential redox balance mediator in cancer chemoprevention. Mediators. Inflamm 6692579.

Chiang, JY. 2009. Bile acids: Regulation of synthesis. J. Lipid. Res. 50:1955–1966.

Chi, Y., Z. Wu, C. Du, M. Zhang, X. Wang, A. Xie, P. Wang, and R. Li. 2023. Regulatory effects mediated by ulvan oligosaccharide and its zinc complex on lipid metabolism in high-fat diet-fed mice. Carbohydrate. Polymers 300:120249.

Collado, M. C., I. S. Surono, J. Meriluoto, and S. Salminen. 2007. Potential probiotic characteristics of Lactobacillus and Enterococcus strains isolated from traditional dadih fermented milk against pathogen intestinal colonization. J. Food Prot 70:700–705.

Comeau, A. M., G. M. Douglas, and MGI. Langille. 2017. Microbiome helper: A custom and streamlined workflow for microbiome research. MSystems 2 e00127-16.

Cufadar, Y., R. Göçmen, G. Kanbur, and B. Yıldırım. 2020. Effects of dietary different levels of nano, organic and inorganic zinc sources on performance, eggshell quality, bone mechanical parameters and mineral contents of the tibia, liver, serum and excreta in laying hens. Biol. Trace. Elem. Res 193:241–251.

Dong, S., J. Ji, L. Hu, and H. Wang. 2019. Dihydromyricetin alleviates acetaminophen-induced liver injury via the regulation of transformation, lipid homeostasis, cell death and regeneration. Life. Sci 227:20–29.

Emami, N. K., U. Jung, B. Voy, and S. Dridi. 2020. Radical response: Effects of heat stress-induced oxidative stress on lipid metabolism in the avian liver. Antioxidants 10:35.

Fan, L., X. Zhao, Q. Tong, X. Zhou, J. Chen, W. Xiong, J. Fang, W. Wang, and C. Shi. 2018. Interactions of dihydromyricetin, a flavonoid from vine tea (Ampelopsis grossedentata) with gut microbiota. J. Food Sci 83:1444–1453.

Forman, H. J., and H. Zhang. 2021. Targeting oxidative stress in disease: promise and limitations of antioxidant therapy. Nat. Rev. Drug Discov 20:689–709.

Franke, T., and U. Deppenmeier. 2018. Physiology and central carbon metabolism of the gut bacterium prevotella copri. Mol. Microbiol 109:528–540.

Furusawa, Y., Y. Obata, S. Fukuda, T. A. Endo, G. Nakato, D. Takahashi, Y. Nakanishi, C. Uetake, K. Kato, T. Kato, M. Takahashi, N. N. Fukuda, S. Murakami, E. Miyauchi, S. Hino, K. Atarashi, S. Onawa, Y. Fujimura, T. Lockett, J. M. Clarke, D. L. Topping, M. Tomita, S. Hori, O. Ohara, T. Morita, H. Koseki, J. Kikuchi, K. Honda, K. Hase, and H. Ohno. 2013. Commensal microbe-derived butyrate induces the differentiation of colonic regulatory T cells. Nature 504:446–450.

Gao, X., P. Liu, C. Wu, T. Wang, G. Liu, H. Cao, C. Zhang, G. Hu, and X. Guo. 2019. Effects of fatty liver hemorrhagic syndrome on the AMP-activated protein kinase signaling pathway in laying hens. Poult. Sci 98:2201–2210.

Gao, S., R. Li, N. Heng, Y. Chen, L. Wang, Z. Li, Y. Guo, X. Sheng, X. Wang, K. Xing, H. Ni, and X. Qi. 2020. Effects of dietary supplementation of natural astaxanthin from Haematococcus pluvialis on antioxidant capacity, lipid metabolism, and accumulation in the egg yolk of laying hens. Poult. Sci 99:5874–5882.

Guo, Z., X. Chen, Z. Huang, D. Chen, B. Yu, H. Chen, J. Yu, H. Yan, P. Zheng, and Y. Luo. 2021. Dietary dihydromyricetin supplementation enhances antioxidant capacity and improves lipid metabolism in finishing pigs. Food Funct 12:6925–6935.

Guo, Z., X. Chen, Z. Huang, D. Chen, B. Yu, J. He, H. Yan, P. Zheng, Y. Luo, J. Yu, and H. Chen. 2022. Effect of dietary dihydromyricetin supplementation on lipid metabolism, antioxidant capacity and skeletal muscle fiber type transformation in mice. Anim. Biotechnol 33:555–562.

Hamid, H., J. Y. Zhang, W. X. Li, C. Liu, M. L. Li, L. H. Zhao, C. Ji, and Q. G. Ma. 2019. Interactions between the cecal microbiota and non-alcoholic steatohepatitis using laying hens as the model. Poult. Sci 98:2509–2521.

Horton, J., J. Goldstein, and M. Brown. 2002. SREBPs: activators of the complete program of cholesterol and fatty acid synthesis in the liver. J. Clin. Invest 109:1125–1131.

HR, J., S. Lee, and SJ. Choi. 2020. Pharmacokinetics and protective effects of tartary buckwheat flour extracts against ethanol-induced liver injury in rats. Antioxidants 9:913.
Khan, S., R. J. Moore, D. Stanley, and KK. Chousalkar. 2020. The gut microbiota of laying hens and its manipulation with prebiotics and probiotics to enhance gut health and food safety. Appl. Environ. Microbiol 86:e00600–e00620.
Kobayashi, T., M. Iwaki, A. Nakajima, A. Nogami, and M. Yoneda. 2022. Current research on the pathogenesis of NAFLD/NASH and the gut-liver axis: gut microbiota, dysbiosis, and leaky-gut syndrome. Int. J. Mol. Sci 23:11689.
Kurdi, P., K. Kawanishi, K. Mizutani, and A. Yokota. 2006. Mechanism of growth inhibition by free bile acids in lactobacilli and bifidobacteria. J Bacteriol 188:1979–1986.
Langille, M. G., J. Zaneveld, J. G. Caporaso, D. McDonald, D. Knights, J. A. Reyes, J. C. Clemente, D. E. Burkepile, R. L. Vega Thurber, R. Knight, R. G. Beiko, and C. Huttenhower. 2013. Predictive functional profiling of microbial communities using 16S rRNA marker gene sequences. Nat. Biotechnol 31:814–821.
Li, S., H. Y. Tan, N. Wang, Z. J. Zhang, L. Lao, C. W. Wong, and Y. Feng. 2015. The role of oxidative stress and antioxidants in liver diseases. Int. J. Mol. Sci 16:26087–26124.
Li, B. Y., H. Y. Li, D. D. Zhou, S. Y. Huang, M. Luo, R. Y. Gan, Q. Q. Mao, A. Saimaiti, A. Shang, and HB. Li. 2021. Effects of different green tea extracts on chronic alcohol induced-fatty liver disease by ameliorating oxidative stress and inflammation in mice. Oxid. Med. Cell Longev 5188205.
Liu, D., Y. Mao, L. Ding, and XA. Zeng. 2019. Dihydromyricetin: A review on identification and quantification methods, biological activities, chemical stability, metabolism and approaches to enhance its bioavailability. Trends Food Sci. Technol 91:586–597.
Lu, M., R. Liu, Z. Chen, C. Su, and L. Pan. 2023. Effects of dietary dihydromyricetin on growth performance, antioxidant capacity, immune response and intestinal microbiota of shrimp (Litopenaeus vannamei). Fish Shellfish Immunol 142:109086.
Luo, F., D. Zeng, W. Wang, Y. Yang, A. Zafar, Z. Wu, Y. Tian, Y. Huang, M. Hasan, and X. Shu. 2021. Bio-conditioning polydihydromyricetin zinc nanoparticles synthesis for advanced catalytic degradation and microbial inhibition. J. Nanostruct Chem 12:903–917.
Matsubara, T., F. Li, and FJ. Gonzalez. 2013. FXR signaling in the enterohepatic system. Mol. Cell Endocrinol 368:17–29.
Meena, J., A. Gupta, R. Ahuja, M. Singh, S. Bhaskar, and A. Panda. 2020. Inorganic nanoparticles for natural product delivery: A review. Environ. Chem. Lett 18:2107–2118.
Mehta, P., R. Shah, S. Lohidasan, and KR. Mahadik. 2015. Pharmacokinetic profile of phytoconstituent(s) isolated from medicinal plants-A comprehensive review. J. Tradit. Complement. Med 5:207–227.
Miao, Y. F., X. N. Gao, D. N. Xu, M. C. Li, Z. S. Gao, Z. H. Tang, N. H. Mhlambi, W. J. Wang, W. T. Fan, X. Z. Shi, G. L. Liu, and SQ. Song. 2021. Protective effect of the new prepared Atractylodes macrocephala Koidz polysaccharide on fatty liver hemorrhagic syndrome in laying hens. Poult. Sci 100:938–948.
Miao, X., P. Luo, J. Liu, J. Wang, and Y. Chen. 2023. Dihydromyricetin ameliorated nonalcoholic steatohepatitis in mice by regulating the composition of serous lipids, bile acids and ileal microflora. Lipids Health Dis 22:112.
National Research Council. 1994. Nutrient Requirements for Poultry. . 9th rev. edn. National Academy Press, Washington DC.
Olechnowicz, J., A. Tinkov, A. Skalny, and J. Suliburska. 2018. Zinc status is associated with inflammation, oxidative stress, lipid, and glucose metabolism. J. Physiol. Sci 68:19–31.
Paroha, S., R. Dewangan, R. Dubey, and P. Sahoo. 2020. Conventional and nanomaterial-based techniques to increase the bioavailability of therapeutic natural products: a review. Environ. Chem. Lett 18:1767–1778.
Patten, D. A., and S. Shetty. 2018. Chronic liver disease: scavenger hunt for novel therapies. Lancet 391:104–105.
Pineda Torra, I., T. Claudel, C. Duval, V. Kosykh, J. C. Fruchart, and B. Staels. 2003. Bile acids induce the expression of the human peroxisome proliferator-activated receptor alpha gene via activation of the farnesoid X receptor. Mol. Endocrinol 17:259–272.
Powell, E., V. Wong, and M. Rinella. 2021. Non-alcoholic fatty liver disease. Lancet 397:2212–2224.
Qi, Y., Z. Zhang, S. Liu, Z. Aluo, L. Zhang, L. Yu, Y. Li, Z. Song, and L. Zhou. 2020. Zinc supplementation alleviates lipid and glucose metabolic disorders induced by a high-fat diet. J. Agr. Food Chem 68:5189–5200.
Rauf, A., A. A. Khalil, U. U. Rahman, A. Khalid, S. Naz, M. A. Shariati, M. Rebezov, E. Z. Urtecho, R. de Albuquerque, S. Anwar, A. Alamri, R. K. Saini, and KRR. Rengasamy. 2022. Recent advances in the therapeutic application of short-chain fatty acids (SCFAs): An updated review. Crit. Rev. Food Sci. Nutr 62:6034–6054.
Rubic, T., G. Lametschwandtner, S. Jost, S. Hinteregger, J. Kund, N. Carballido-Perrig, C. Schwärzler, T. Junt, H. Voshol, J. G. Meingassner, X. Mao, G. Werner, A. Rot, and JM. Carballido. 2008. Triggering the succinate receptor GPR91 on dendritic cells enhances immunity. Nat. Immunol 9:1261–1269.
Russell, DW. 2003. The enzymes, regulation, and genetics of bile acid synthesis. Annu. Rev. Biochem 72:137–174.
Shi, C., J. Wang, R. Zhang, M. Ishfaq, Y. Li, R. Zhang, C. Si, R. Li, C. Li, and F. Liu. 2022. Dihydromyricetin alleviates Escherichia coli lipopolysaccharide-induced hepatic injury in chickens by inhibiting the NLRP3 inflammasome. Vet. Res 53:6.
Shini, A., S. Shini, and W. Bryden. 2019. Fatty liver haemorrhagic syndrome occurrence in laying hens: Impact of production system. Avian Pathol. 48:25–34.
Silva, J., X. Yu, R. Moradian, C. Folk, M. H. Spatz, P. Kim, A. A. Bhatti, D. L. Davies, and J. Liang. 2020. Dihydromyricetin protects the liver via changes in lipid metabolism and enhanced ethanol metabolism. Alcohol. Clin. Exp. Res 44:1046–1060.
Song, Z., A. Xiao, and F. Yang. 2018. Regulation and metabolic significance of de novo lipogenesis in adipose tissues. Nutrients 10:1383.
Song, Y., L. Sun, P. Ma, L. Xu, and P. Xiao. 2022. Dihydromyricetin prevents obesity via regulating bile acid metabolism associated with the farnesoid X receptor in ob/ob mice. Food Funct 13:2491–2503.
Sorosh, Z., S. Salari, M. Sari, J. Fayazi, and S. Tabatabaei. 2019. Dietary zinc supplementation and the performance and behaviour of caged laying hens. Anim. Product. Sci. 59:331–337.
Trebicka, J., P. Bork, A. Krag, and M. Arumugam. 2021. Utilizing the gut microbiome in decompensated cirrhosis and acute-on-chronic liver failure. Nat. Rev. Gastroenterol. Hepatol 18:167–180.
Trott, K. A., F. Giannitti, G. Rimoldi, A. Hill, L. Woods, B. Barr, M. Anderson, and A. Mete. 2014. Fatty liver hemorrhagic syndrome in the backyard chicken: A retrospective histopathologic case series. Vet. Pathol 51:787–795.
Tu, W., Y. Zhang, K. Jiang, and S. Jiang. 2023. Osteocalcin and its potential functions for preventing fatty liver hemorrhagic syndrome in Poultry. Animals 13:1380.
Turnbaugh, P. J., R. E. Ley, M. A. Mahowald, V. Magrini, E. R. Mardis, and JI. Gordon. 2006. An obesity-associated gut microbiome with increased capacity for energy harvest. Nature 444:1027–1031.
Vanti, G. 2021. Recent strategies in nanodelivery systems for natural products: a review. Environ. Chem. Lett 19:4311–4326.
Wang, R., Y. Ren, J. Hafiz Umer, J. Luo, M. Zhou, and X. Shu. 2022. Effect of different dietary zinc sources on growth, element deposition, antioxidation, lipid metabolism, and related gene expression in hybrid grouper (♀ Epinephelus fuscoguttatus × ♂ E. lanceolatus). Aquacult. Nutr 1:8371440.
Wang, W. W., J. Wang, H. J. Zhang, S. G. Wu, and GH. Qi. 2020. Supplemental clostridium butyricum modulates lipid metabolism through shaping gut microbiota and bile acid profile of aged laying hens. Front. Microbiol. 11:600.
Wassie, T., X. Duan, C. Xie, R. Wang, and X. Wu. 2022. Dietary Enteromorpha polysaccharide-Zn supplementation regulates amino acid and fatty acid metabolism by improving the antioxidant activity in chicken. J. Anim. Sci. Biotechnol 13:18.
Wu, C., X. Zheng, and L. Chen. 2011. Study on antioxidant activity of dihydromyricetin-zinc(II) complex. AMR 183:863–867.
Wu, J., Z. Xiao, H. Li, N. Zhu, J. Gu, W. Wang, C. Liu, W. Wang, and L. Qin. 2022. Present status, challenges, and prospects of dihydromyricetin in the battle against cancer. Cancers 14:3487.

Xie, C., Z. Chen, C. Zhang, X. Xu, J. Jin, W. Zhan, T. Han, and J. Wang. 2016. 2016. Dihydromyricetin ameliorates oleic acid-induced lipid accumulation in L02 and HepG2 cells by inhibiting lipogenesis and oxidative stress. Life. Sci 157:131–139.

Xing, C., Y. Wang, X. Dai, F. Yang, J. Luo, P. Liu, C. Zhang, H. Cao, and G. Hu. 2020. The protective effects of resveratrol on antioxidant function and the mRNA expression of inflammatory cytokines in the ovaries of hens with fatty liver hemorrhagic syndrome. Poult. Sci 99:1019–1027.

Xu, M., K. Luo, J. Li, Y. Li, Y. Zhang, Z. Yuan, Q. Xu, and X. Wu. 2022. Role of intestinal microbes in chronic liver diseases. Int. J. Mol. Sci. 23:12661.

Yang, Y., W. He, L. Huang, R. Wang, X. Shu, and Y. Tian. 2022. Effects of different zinc sources on performance, serum biochemical indexes and microelement deposition of laying hens. Chin. J. Anim. Nutr. 34:2393–2402. https://kns.cnki.net/kcms/detail/11.5461.s.20220124.1104.019.html.

Younossi, Z. M., S. Zelber-Sagi, L. Henry, and L. H. Gerber. 2023. Lifestyle interventions in nonalcoholic fatty liver disease. Nat. Rev. Gastroenterol. Hepatol 20:708–722.

Zeng, Y., Y. Q. Hua, W. Wang, H. Zhang, and XL. u. 2020. Modulation of SIRT1-mediated signaling cascades in the liver contributes to the amelioration of nonalcoholic steatohepatitis in high fat fed middle-aged LDL receptor knockout mice by dihydromyricetin. Biochem. Pharmacol 175:113927.

Zhang, J., J. S. Brodbelt, and J. Wang. 2005. Threshold dissociation and molecular modeling of transition metal complexes of flavonoids. J. Am. Soc. Mass. Spectrom 16:139–151.

Zhang, W., Y. Zhao, F. Li, L. Li, Y. Feng, L. Min, D. Ma, S. Yu, J. Liu, H. Zhang, T. Shi, F. Li, and W. Shen. 2018. Zinc oxide nanoparticle caused plasma metabolomic perturbations correlate with hepatic steatosis. Front. Pharmacol. 9:57.

Zhang, R., H. Zhang, H. Shi, D. Zhang, Z. Zhang, and H. Liu. 2022. Strategic developments in the drug delivery of natural product dihydromyricetin: Applications, prospects, and challenges. Drug Deliv 29:3052–3070.

Zhao, Y., L. Li, P. Zhang, X. Liu, W. Zhang, Z. Ding, S. Wang, W. Shen, L. Min, and Z. Hao. 2016. Regulation of egg quality and lipids metabolism by zinc oxide nanoparticles. Poult. Sci 95:920–933.

Zhou, D. D., Q. Q. Mao, B. Y. Li, A. Saimaiti, S. Y. Huang, R. G. Xiong, A. Shang, M. Luo, H. Y. Li, R. Y. Gan, H. B. Li, and S. Li. 2022. Effects of different green teas on obesity and non-alcoholic fatty liver disease induced by a high-fat diet in mice. Front. Nutr 9:929210.

Zhu, Y. W., W. X. Li, L. Lu, L. Y. Zhang, C. Ji, X. Lin, H. C. Liu, J. Odle, and X. G. Luo. 2017. Impact of maternal heat stress in conjunction with dietary zinc supplementation on hatchability, embryonic development, and growth performance in offspring broilers. Poult. Sci 96:2351–2359.